CANTERA Simulations of Water-Laden Methane/Air Nonpremixed Counterflow Flames

V. Ricchiuti[a], R. E. Padilla[b], S.Karnani[b], and D. Dunn-Rankin[b]

[a]*Aerospace Sciences and Technology Department, Polytechnic University of Milan, Milan, Italy, 20156*
[b]*Department of Mechanical and Aerospace Engineering, University of California, Irvine, CA 92697, USA*

Submitted to: The 8th US National Combustion Meeting

Colloquium: Reaction kinetics

Address for correspondence: Derek Dunn-Rankin

University of California, Irvine

Department of Mechanical and Aerospace Engineering

4200 Engineering Gateway

Irvine, CA 92697-3975, USA

CANTERA Simulations of Water-Laden Methane/Air Nonpremixed Counterflow Flames

V. Ricchiuti[a], R. E. Padilla[b], S.Karnani[b], and D. Dunn-Rankin[b]

[a]*Aerospace Sciences and Technology Department, Polytechnic University of Milan, Milan, Italy, 20156*
[b]*Department of Mechanical and Aerospace Engineering, University of California, Irvine, CA 92697, USA*

Abstract

The direct combustion of methane hydrates occurs as a non-premixed flame driven by natural convection. The methane released from the hydrate is accompanied by large quantities of water vapor. Qualitative experiments indicate that hydrate flames can be sustained with approximately 2 moles of water per mole of methane entering the reaction zone. Very little information, however, is available on combustion at such highly humidified conditions. To analyze this combustion process, we use CANTERA, an open source chemical kinetics program, to simulate combustion in an opposed flow configuration, where air is introduced on one side and a preheated mixture of water vapor/methane is on the other. The study has three parts. First, we use GRI Mech 3.0 and determine the water level at which the flame cannot be sustained for different inlet gas temperatures. Next, we compare results from the full mechanism to those from a smaller set of reactions that do not include nitrogen species. Finally, we evaluate the details of the kinetics to determine the role of thermal factors and chemical factors limiting the water level at extinguishment. The results show that water's role in preferentially promoting endothermic reactions may be responsible for limiting chain initiating, propagating, and branching reactions which ultimately leads to flame extinguishment.

1. Introduction

In recent years there has been a renewed interest in the study of methane hydrates (clathrates) because of their capability of storing methane at high density and because they represent a very important potential resource of clean energy, that in the future could supply a significant level of natural gas in the world. The structure of methane hydrates is quite similar to ice, but there is a substantial difference: in the polyhedral crystal lattice of the hydrate, where molecules of water are orderly disposed, there is some space in which methane molecules are trapped. A fully saturated clathrate contains about 85% water (H_2O) and 15% methane (CH_4,). Despite this large amount of water, experiments[1] show that a flame can be sustained when hydrates are burned in air; though while burning, the methane fuel is diluted heavily with water vapor.

The aim of this work is to better understand, through numerical simulations, the combustion process of clathrates, focusing on the reaction mechanism of methane (fuel) diluted with water vapor burning in air; in particular, flame temperature and flammability limits (i.e., the maximum amount of water that can be added before the flame can no longer burn) is explored along with an analysis of what triggers the transition to extinguishment in a water-laden methane/air diffusion flame.

Numerical simulations have been performed using Cantera[2], an open source chemical-kinetics solver to calculate the combustion of methane and water vapor in air; because water and methane are trapped together into clathrates, a non-premixed counterflow configuration has been used. As shown in Figure 1[1], the configuration consists in a burner with two nozzles positioned on opposite sides: the bottom one ejects water vapor introduced into preheated methane fuel stream, and the top one ejects an air stream. It is a theoretically 1D configuration. As in other combustion problems, natural convection driven clathrate combustion can be approximately represented by a turbulent or unsteady laminar non-premixed flame, which in turn can be considered as an ensemble of one-dimensional laminar flamelets, and these can be modeled in a counterflow non-premixed configuration[1]. In this geometrically simplified system, all mixture properties depend only on the axial direction x[3]. However, this is a simplification of what really happens in clathrate combustion, where the dependence of some parameters on the radial direction r cannot be neglected; this can explain some of the differences between numerical simulations and experiments (even idealized counterflow flame experiments), such as why the flame temperature computed with Cantera is always higher than the measured ones (it is likely that part of the discrepancy comes from radial variations and radiation heat losses that have not been taken into account in the Cantera simulations).

2. Numerical simulations

Simulations with Cantera have been performed in order to determine the maximum amount of water (typically described in the ratio of moles of water/moles of methane) that can be added before a counterflow flame can no longer burn and to develop an analysis of the chemical kinetic processes that dominate the combustion of water-laden fuel/air non-premixed flames in the counterflow configuration.

3. Results and Discussion

3.1. GRI3.0 mechanism (full mechanism)

GRI-Mech 3.0[4] is an optimized mechanism designed to model natural gas combustion, including NO formation and re-burn chemistry; the optimization process is designed to provide sound basic kinetics which also furnish the best combined modeling predictability of basic combustion properties. It includes four elements (H, N, O, C), 53 species and 325 reactions; there are different types of reactions: reversible and irreversible, three-body and fall-off (in which the rate constant depends on pressure: the presence of third body is fundamental only at low pressure, at high pressure reactions proceed also without it). The last two reaction types are of the form:

$$A + B + M \Leftrightarrow AB + M$$

where M is the third body (indicated as (M) for fall-off); efficiency ε of species that act as a third body must be specified, otherwise it is automatically set to one. Physically, collision efficiency represents the capability of a molecule to subtract energy from the forward reaction and to add energy to the reverse reaction.

For each reaction, pre-exponential factor A, coefficient n (that indicates the temperature dependence) and activation energy E_a are specified, in order to compute the rate constant according to the Arrhenius function:

$$k_f(T) = AT^n \exp\left(-\frac{\mathrm{E_a}}{\mathrm{RT}}\right)$$

The mechanism includes thermal[5] and transport[6] properties, for each species: the former contains the NASA polynomial coefficients that are used to compute the molar heat capacity at constant pressure $\frac{c_p^0(T)}{T}$, the molar enthalpy $\frac{h^0(T)}{RT}$ and the absolute molar entropy $\frac{s_p^0(T)}{T}$ (apex "0" indicates standard conditions); the latter include physical properties of molecules such as geometry, diameter, well depth, dipole moment, polarizability and rotational relaxation collision time.

The following initial conditions have been considered:

- Pressure: 1 atm;
- Fuel volumetric flow rate: 3 $\frac{L}{min}$;

- Oxidizer volumetric flow rate: $6\ \frac{L}{min}$;
- Top and bottom nozzle diameter: $d = 0.019\ m$;
- Nozzles distance: $l = 0.0127\ m$;
- Fuel initial temperature: $T_{f,in} = 550\ K, T_{f,in} = 720\ K$;
- Oxidizer initial temperature: $T_{ox,in} = 298\ K$;
- Fuel initial composition:

$$\begin{cases} CH_4 = 1\ mol,\ \ H_2O = (0, 0.1, 0.2, 0.3, 0.4, 0.48)\ mol & (T_{f,in} = 550\ K) \\ CH_4 = 1\ mol,\ \ H_2O = (0, 0.1, 0.2, 0.3, 0.4, 0.5, 0.7, 1, 1.1, 1.2)\ mol & (T_{f,in} = 720\ K) \end{cases}$$

- Oxidizer initial composition: $O_2 = 0.21\ mol,\ N_2 = 0.78\ mol,\ Ar = 0.01\ mol$.

These conditions were selected to approximate a typical condition in an experimental campaign that is underway in parallel with this study. More cases are run with a higher fuel inlet temperature because the higher the fuel inlet temperature, the higher the maximum amount of H_2O that can be added; the reason is that as temperature increases, the decomposition of water (that is what starts the kinetic process, through the creation of a pool of radicals such as H, O, OH, HO_2, H_2O_2) is easier. Figure 2 and Figure 3 show the spatial variation of flame temperature; Figure 4 and Figure 5 represent the axial velocity of the mixture spatially. These results are very similar to those found in the similar study of Suh and Atreya[7], though the water addition in their case was on the air side of the counterflow flame. As shown, the flame is always located on the fuel side of the symmetric plane and on the oxidizer side of stagnation plane (where the axial velocity is null), no matter the initial amount of H_2O; this is because flame resides very close to the location where the mixture reaches stoichiometric conditions, which for the considered case occurs when the molar fraction of fuel to oxidizer is around 10%.

The drastic drops in both temperature profiles for the case of non ignition after a very small change in the amount of added water suggests that chemistry dominates over thermal effects[7]; in fact, if the combustion process had been controlled only by thermal sinks, there would be a more graduate decrease of temperature, for increasing amounts of water. It is still possible, however, that a small thermal sink effect of the water could reduce the overall reaction temperature sufficiently to create extinction. To further explore this effect, simulations for the addition of "fake Ar" (instead of water) to fuel side have been performed; fake Ar is actually a non-reacting water; that is, it has the same thermal properties of water, in terms of NASA polynomial coefficients and the same third body efficiency. Figure 6, 7, 8 and 9 show temperature and axial velocity profiles for this case; it can be seen that the amount of fake Ar that can be added to the fuel before extinction is much higher than for the case of water addition, for both $T_{in,f}$=550 K and $T_{in,f}$.=720 K. Because these results are so different (also in terms of molar fraction of some produced species such as

CH_2O, CH_3, H_2O_2, OH), it seems clear that chemistry is the dominating factor in the near-limit combustion of water-laden methane/air non-premixed flame in a counterflow configuration.

3.2. Reduced model

GRI3.0 is a very detailed mechanism that can simulate many combustion mechanisms; however, it is difficult to manage such a high number of equations and species when chemical kinetics analysis is required. For this reason, a reduced model[8] based on the GRI mechanism has been considered; this model does not take into account species formed by molecular nitrogen such as NO_x. It includes 4 elements (H, O, C, N), 31 species and 104 equations; as shown by Figures 10-17, for the non-premixed counterflow configuration this reduced model gives results that are very similar to the ones obtained with full mechanism, for the same initial conditions. For this reason, chemical kinetics analysis has been performed using the reduced model.

3.3. Chemical kinetic analysis

In order to understand the reasons why flame can no longer burn at a critical addition of water vapor, an analysis of the influence of some chemical kinetic parameters on species and reactions of the reduced model has been performed. Given a generic reaction:

$$\sum_{j=1}^{n} \upsilon'_{j,i} \; M_{j,i} \Leftrightarrow \sum_{j=1}^{n} \upsilon''_{j,i} \; M_{j,i} \qquad j = 1{:}\,n, i = 1{:}\,m$$

where *n* is the number of species into reaction *i*, *m* is the number of reactions, $\upsilon'_{j,i}$ and $\upsilon''_{j,i}$ are respectively the stoichiometric coefficients of reactants and products, the following parameters can be defined:

- Order of the reaction: $\begin{cases} n_{f,i=} \sum_{j=1}^{n} \upsilon'_{j,i} \\ n_{r,i=} \sum_{j=1}^{n} \upsilon''_{j,i} \end{cases}$
- Forward rate constant: $k_{f,i}(T) = A_i T^{n_i} \exp\left(-\frac{\mathrm{E_{a,i}}}{\mathrm{RT}}\right)$
- Forward, reverse and net rates of progress: $\begin{cases} Q_{f,i} = k_{f,i} \prod_{j=1}^{n} [M_j]^{\upsilon'_{j,i}} \\ Q_{r,i} = k_{b,i} \prod_{j=1}^{n} [M_j]^{\upsilon''_{j,i}} \\ NRP_i = Q_{f,i} - Q_{r,i} \end{cases}$

  These are properties related to the reactions; units are: $\frac{kmol}{m^3\, s}$
- Matrix of products stoichiometric coefficients: N_p; it is a *(n,m)* matrix, where the (*j,i*) element is the stoichiometric coefficient of species *j*, as product, in reaction *i*
- Matrix of reactants stoichiometric coefficients: N_r; it is a *(n,m)* matrix, where the (*j,i*) element is the stoichiometric coefficient of species *j*, as reactant, in reaction *i*

- Creation, destruction and net production rates: $\begin{cases} C_{r,j}=\sum_{i=1}^{m}(\mathrm{Np_{j,i}}\ Q_{f,i}+\mathrm{Nr_{j,i}}\ Q_{r,i}) \\ D_{r,j}=\sum_{i=1}^{m}(\mathrm{Nr_{j,i}}\ Q_{f,i}+\mathrm{Np_{j,i}}\ Q_{r,i}) \\ NPR_j = C_{r,j} - D_{r,j} \end{cases}$

  These are properties related to species; they take into account the contribution of each reaction to their creation or destruction; units: $\frac{kmol}{m^3\ s}$

- Enthalpy variation: $\Delta H_i = \Delta H_{products,i} - \Delta H_{reactants,i}$; units: $\frac{J}{kmol}$.

Basing on these definitions, if NRP_i is positive equilibrium of reaction *i* is shifted towards the right (it proceeds mainly in the forward direction); while if it's negative, equilibrium of reaction *i* is shifted towards the left (it proceeds mainly in the reverse direction). So, the sign of NRP_i has been used to determine if a reaction is endothermic or exothermic; in fact, the ΔH given by Cantera is computed supposing that reactions always occur in the forward direction. So:

- If $NRP_i > 0$, ΔH given by Cantera can be interpreted without change;
- If $NRP_i < 0$, ΔH given by Cantera needs a negative sign.

Some of the reactions included in the reduced model belong to basic reaction paths[9]**:**

a) CH_4 – air, low temperature
b) CH_4 – air, high temperature
c) H_2 – O_2
d) CO – O_2
e) Higher order hydrocarbons

All the others can be considered as the result of the interaction among these previous mechanisms; they will be called combined reaction paths in the discussion that follows. Simulations have been performed only for the more experimentally relevant case of $T_{f,in} = 550\ K$.

Results reported in the following paragraphs reflect the global behavior of the system, because they have been obtained from integration of kinetic parameters along the grid that represents the mono dimensional domain of the problem; if a local analysis is performed, results can be quite different.

3.3.1. H_2O addition on the fuel side

When increasing amounts of water are added on the fuel side, the process continues to be globally exothermic: $\Delta H_{tot} = -1.5856 * 10^8 \frac{J}{kmol}$. The reasons why extinction occurs are that additional water:

- shifts the equilibrium of some reactions in such a way that their ΔH_i becomes positive; so, in the basic reaction paths these reactions are inverted: they mainly proceed in the opposite direction with respect to the way they are written;
- does not allow important reactions to occur anymore.

The most important inverted reactions, in terms of ΔH, are:

b) $\{38)\ H + CH_2O + (M) \rightharpoonup CH_3O + (M) \quad \Delta H_{38} = -1.1995 * 10^6 \frac{J}{kmol} \quad (supposed\ path: "\leftharpoondown")$

c) $\begin{cases} 1)\ H + O + M \leftharpoondown OH + M & \Delta H_1 = 5.4479 * 10^6 \frac{J}{kmol} \quad (chain\ terminating: "\rightharpoonup") \\ 49)\ H_2 + OH \leftharpoondown H + H_2O & \Delta H_{49} = 0.8064 * 10^6 \frac{J}{kmol} \quad (chain\ branching: "\rightharpoonup") \\ 53)\ OH + H_2O_2 \leftharpoondown H_2O + HO_2 & \Delta H_{53} = 1.6909 * 10^6 \frac{J}{kmol} \quad (supposed\ path: "\rightharpoonup") \end{cases}$

e) $\begin{cases} 64)\ OH + C_2H_4 \leftharpoondown H_2O + C_2H_3 & \Delta H_{64} = 0.4285 * 10^6 \frac{J}{kmol} \quad (supposed\ path: "\rightharpoonup") \\ 104)\ O_2 + C_2H_5 \leftharpoondown HO_2 + C_2H_4 & \Delta H_{104} = 0.6822 * 10^6 \frac{J}{kmol} \quad (supposed\ path: "\rightharpoonup") \end{cases}$

f) Also some of the combined paths are inverted:

$\begin{cases} 5)\ O + CH_2(S) \leftharpoondown H + HCO & \Delta H_5 = 5.3209 * 10^6 \frac{J}{kmol} \\ 10)\ O + HCO \leftharpoondown H + CO_2 & \Delta H_{10} = 5.9221 * 10^6 \frac{J}{kmol} \end{cases}$

Reactions that do not occur are:

e) $\begin{cases} 47)\ H + C_2H_6 \rightharpoonup H_2 + C_2H_5 & \Delta H_{47} = -0.1920 * 10^6 \frac{J}{kmol} \quad (supposed\ path: "\rightharpoonup") \\ 65)\ OH + C_2H_6 \rightharpoonup H_2O + C_2H_5 & \Delta H_{65} = -0.9985 * 10^6 \frac{J}{kmol} \quad (supposed\ path: "\rightharpoonup") \end{cases}$

f) $\begin{cases} 16)\ O + C_2H_6 \rightharpoonup OH + C_2H_5 & \Delta H_{16} = -0.0886 * 10^6 \frac{J}{kmol} \\ 46)\ H + C_2H_5 + (M) \rightharpoonup C_2H_6 + (M) & \Delta H_{46} = -5.3593 * 10^6 \frac{J}{kmol} \\ 97)\ CH_3 + C_2H_6 \rightharpoonup CH_4 + C_2H_5 & \Delta H_{97} = -0.2469 * 10^6 \frac{J}{kmol} \end{cases}$

All these considerations explain why there is a drastic drop of temperature: above the initial amount of $0.4\ mol$, water strongly modifies the chemistry of the whole process by inverting or stopping important reaction paths; physically, what happens is that the system does not release enough energy (because part of it is absorbed by reactions that have become endothermic and part of it was supposed to come from the exothermic reactions that no longer occur) to sustain a stable flame.

3.3.2. Ar_{fake} addition on the fuel side

Similarly to what happens for water, also extinction due to fake Ar addition on the fuel side occurs even if the process remains globally exothermic: $\Delta H_{tot} = -6.8840 * 10^7 \frac{J}{kmol}$; extinction occurs because additional fake Ar shifts the equilibrium of some reactions in the endothermic direction and does not let some important reaction paths proceed. However, a comparison of the case of non-ignition for water and fake Ar addition on the fuel side shows that reactions that are inverted or do not occur are different; these two species affect the chemistry near extinction in a very different way.

The most important inverted reactions, in terms of ΔH, are:

a) $\{91)\ H_2O_2 + CH_3 \rightharpoonup HO_2 + CH_4 \quad \Delta H_{91} = -0.9416 * 10^6 \frac{J}{kmol} \quad (chain\ propagating: "\leftharpoondown")$

c) $\begin{cases} 3)\ O + HO_2 \leftharpoondown O_2 + OH & \Delta H_3 = 2.8230 * 10^6 \frac{J}{kmol} \quad (supposed\ path: " \rightharpoonup ") \\ 29)\ H + OH + M \leftharpoondown H_2O + M & \Delta H_{29} = 6.3614 * 10^6 \frac{J}{kmol} \quad (chain\ terminating: " \rightharpoonup ") \\ 52)\ OH + HO_2 \leftharpoondown O_2 + H_2O & \Delta H_{52} = 3.7336 * 10^6 \frac{J}{kmol} \quad (supposed\ path: " \rightharpoonup ") \end{cases}$

e) $\{65)\ OH + C_2H_6 \leftharpoondown H_2O + C_2H_5 \quad \Delta H_{65} = 0.9984 * 10^6 \frac{J}{kmol} \quad (supposed\ path: " \rightharpoonup ")$

f) Also some of the combined paths are inverted:

$$\begin{cases} 33)\ H + CH_2 + (M) \leftharpoondown CH_3 + (M) & \Delta H_{33} = 5.9067 * 10^6 \frac{J}{kmol} \\ 68)\ HO_2 + CH_2 \leftharpoondown OH + CH_2O & \Delta H_{68} = 6.0278 * 10^6 \frac{J}{kmol} \end{cases}$$

Some of the reactions that do not occur are:

b) $\{39)\ H + CH_2O \rightharpoonup H_2 + HCO \quad \Delta H_{39} = -0.8488 * 10^6 \frac{J}{kmol} \quad (supposed\ path: " \rightharpoonup ")$

c) $\begin{cases} 19)\ H + O_2 + M \rightharpoonup HO_2 + M & \Delta H_{19} = -2.6278 * 10^6 \frac{J}{kmol} \quad (supposed\ path: " \rightharpoonup ") \\ 25)\ 2H + M \rightharpoonup H_2 + M & \Delta H_2 = -5.5542 * 10^6 \frac{J}{kmol} \quad (chain\ terminating: " \rightharpoonup ") \end{cases}$

d) $\{71)\ HO_2 + CO \rightharpoonup OH + CO_2 \quad \Delta H_{71} = -3.2477 * 10^6 \frac{J}{kmol} \quad (supposed\ path: " \rightharpoonup ")$

e) $\{45)\ H + C_2H_4 \rightharpoonup H_2 + C_2H_3 \quad \Delta H_{45} = +0.3791 * 10^6 \frac{J}{kmol} \quad (supposed\ path: " \rightharpoonup ")$

f) $\begin{cases} 37)\ H + HCO \rightharpoonup H_2 + CO & \Delta H_{37} = -4.7042 * 10^6 \frac{J}{kmol} \\ 43)\ H + C_2H_3 \rightharpoonup H_2 + C_2H_2 & \Delta H_{43} = -3.6663 * 10^6 \frac{J}{kmol} \end{cases}$

It can be noticed that some of these inverted reactions are of the three-body or fall-off type; this happens because water and fake Ar chemically (and not thermally) behave differently.

Therefore, for fake Ar the drastic drop of temperature occurs because additions above the initial amount of $2.8\ mol$ strongly modifies the chemistry of the process by inverting or stopping important reaction paths; physically, as for the water case what happens is that the system does not release enough energy (because part of it is absorbed by reactions that have become endothermic and part of it was supposed to come from the exothermic reactions that do not occur anymore) to sustain a stable flame. But, as mentioned before, the detailed effects of fake Ar on the chemistry of the extinction process are very different from those identified for the case of water.

3.3.3. H_2O addition on air side

Simulations have been performed also for the case of water addition on the air side; as shown in Figures 18-19 (GRI3.0) and 20-21 (reduced model), extinction occurs when an initial amount of about $0.2\ mol$ of water is added, for $T_{f,in} = 550\ K$. Chemical kinetic analysis shows that, for this amount of water on the air side, the system is still globally exothermic: $\Delta H_{tot} = -1.7093 * 10^8 \frac{J}{kmol}$. The reasons that the flame does not burn are different from the ones explained in Paragraph *3.3.1;*

in fact, the reason why extinction occurs now is that additional water shifts the equilibrium of some reactions in the exothermic direction. Comparing the cases of extinction for water addition on the fuel and air side, the most important inverted reactions, in terms of ΔH, are:

a) $\left\{91)\ H_2O_2 + CH_3 \rightharpoondown HO_2 + CH_4 \quad \Delta H_{91} = -0.9395 * 10^6 \frac{J}{kmol} \quad (chain\ propagating: "\leftharpoondown")\right.$

b) $\left\{89)\ O_2 + CH_3 \leftharpoondown O + CH_3O \quad \Delta H_{89} = -1.5001 * 10^6 \frac{J}{kmol} \quad (supposed\ path: "\rightharpoondown")\right.$

c) $\left\{32)\ H + H_2O_2 \rightharpoondown H_2 + HO_2 \quad \Delta H_{32} = -0.8845 * 10^8 \frac{J}{kmol} \quad (supposed\ path: "\leftharpoondown")\right.$

d) $\left\{71)\ HO_2 + CO \leftharpoondown OH + CO_2 \quad \Delta H_{71} = 3.2486 * 10^6 \frac{J}{kmol} \quad (supposed\ path: "\rightharpoondown")\right.$

f) Also some of the combined reaction paths are inverted:

$$\begin{cases} 5)\ O + CH_2(S) \rightharpoondown H + HCO & \Delta H_5 = -5.3209 * 10^6 \frac{J}{kmol} \\ 10)\ O + HCO \rightharpoondown H + CO_2 & \Delta H_{10} = -5.9221 * 10^8 \frac{J}{kmol} \\ 101)\ O_2 + CH_3O \leftharpoondown HO_2 + CH_2O & \Delta H_{101} = -1.4252 * 10^8 \frac{J}{kmol} \end{cases}$$

So, an initial amount of water higher than the above-mentioned shifts the equilibrium of some reaction paths in such a way that their ΔH_i becomes negative; even if the system releases all the energy it produces, ignition does not occur. Moreover, an analysis of the NPR_j shows that a pool of CH_3 is created. It is possible that, because water and fuel are injected from opposite sides of the burner, water radicals cannot recombine with methane radicals to encourage combustion.

4. Conclusions

Simulations performed with Cantera show that chemistry is the dominating factor in the extinguishment of water laden methane/air non premixed flames in a counterflow configuration; it can be said that:

I. water added on the fuel side behaves mainly as a thermal sink, because when extinction occurs most (about 85%) of the heat released by the system is lost into heating the ambient; however, there is a small amount (15%) of this heat that is absorbed by the system in order to shift the equilibrium of some reactions in the endothermic direction. And the inversion of these reactions, in addition to the arrest of some other reaction paths, is a chemical effect. So, chemistry dominates over thermal effects near extinction;

II. fake Ar behaves like a thermal sink too; when extinction occurs, about 80% of heat released by the system is lost into heating he ambient, but the remaining 20% is absorbed by the system itself to invert some reactions and make them endothermic. And this effect, together with the block of some reaction paths, is a chemical effect; again, chemistry dominates over thermal effects near extinction. But, as described before, the effects of fake Ar on the chemistry of the non-ignition process are different from those identified for the water case;

III. water added on the air side behaves as a thermal sink because extinction occurs when the process is still exothermic; but differently from what happens for water addition on the fuel side, the inverted reactions contribute (in the amount of about 5%) to the total energy release; lack of ignition occurs because important reaction paths are inverted and not because there is not enough energy release. So, again, extinction is controlled by the chemistry.

In addition to the self-contained findings listed above, comparisons with experimental results[1],[7] show that temperature obtained with Cantera is always higher (about 200K) than those measured and the heated zone is narrower. While all of the reasons for this discrepancy are not yet identified, it is likely the result of the ideal one-dimensional nature of the simulation where the actual system has some unsteadiness and non-ideal mixing. Moreover, the model does not take into account heat losses; while in the experiments radiation heat losses are always present. The higher temperature and narrower profile might also indicate a higher strain rate in the calculation than in the experiment. The work of Smooke et al.[3] is a similar comparison between counterflow experiments and calculations, except that the dilution of the fuel is with nitrogen rather than water. In their case, the experimental temperature and calculated temperature were much closer together, indicating that with careful treatment of strain rate and boundary conditions improvements are possible.

Some differences can be noticed also in the initial amount of moles of water that cause extinction of the flame: with the above-mentioned initial conditions in terms of volumetric flow rates, it occurs when molar fraction of water to methane is around 0.5 ($T_{f,in} = 550\ K$) and 1.2 ($T_{f,in} = 720\ K$); while experiments[1] show that flame can be sustained till the molar fraction of water to methane is around 2. This is due to the initial conditions: if both fuel and oxidizer flow rates are decreased of about the half, computed and experimental results are in agreement. This is another indication of the influence of strain rate on the findings.

References

[1] O.C. Kwon, S. Lee, R. Padilla, D. Dunn-Rankin, T. Pham, *Extinction limits and structure of counterflow nonpremixed water-laden methane/air flame*, W2P117- Work-in-Progress Poster, International Combustion Symposium, Warsaw, Poland, July 30-August 3

[2] Cantera Developers (2012). Cantera: Chemical kinetics, Thermodynamics, Transport properties. [Online]. Available: http://cantera.github.com/docs/sphinx/html/index.html

[3] M. D. Smooke, I. K. Puri, K. Seshadri, *A comparison between numerical calculations and experimental measurementsof the structure of a counterflow diffusion flame burning diluted methane in diluted air*, Twenty-first Symposium (International) on Combustion/The Combustion Institute (1986), pp. 1783-1792

[4] Gas Research Institute. Gri-Mech™. [Online]. Available:http://www.me.berkeley.edu/gri_mech/version30/text30.html

[5] Cantera Developers (2012). Cantera: Chemical kinetics, Thermodynamics, Transport properties – Elements and Species. [Online]. Available: http://cantera.github.com/docs/sphinx/html/cti/species.html

[6] Cantera Developers (2012). Cantera: Chemical kinetics, Thermodynamics, Transport properties – CTI Class Reference . [Online]. Available: http://cantera.github.com/docs/sphinx/html/cti/classes.html#transport-properties

[7] Jaeil Suh, Arvind Atreya, *The effect of water vapor on counterflow diffusion flames,* International Conference on Fire Research and Engineering, Orlando, FL (1995), pp. 103-108

[8] Andrei Kazakov and Michael Frenklach. Reduced Reaction Sets based on GRI- Mech 1.2. [Online]. Available: http://www.me.berkeley.edu/drm/

[9] Irvin Glassman, Richard Y. Yetter, *Combustion*, *4*th Edition, Academic Press

List of figures

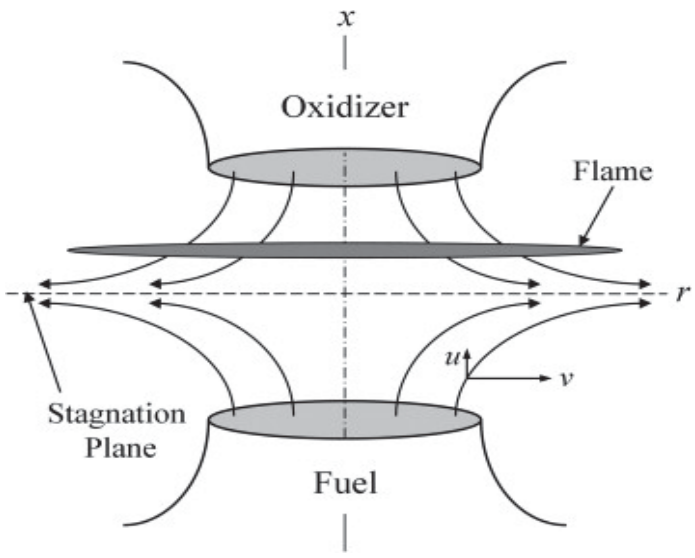

Figure 1: Scheme of a counterflow configuration

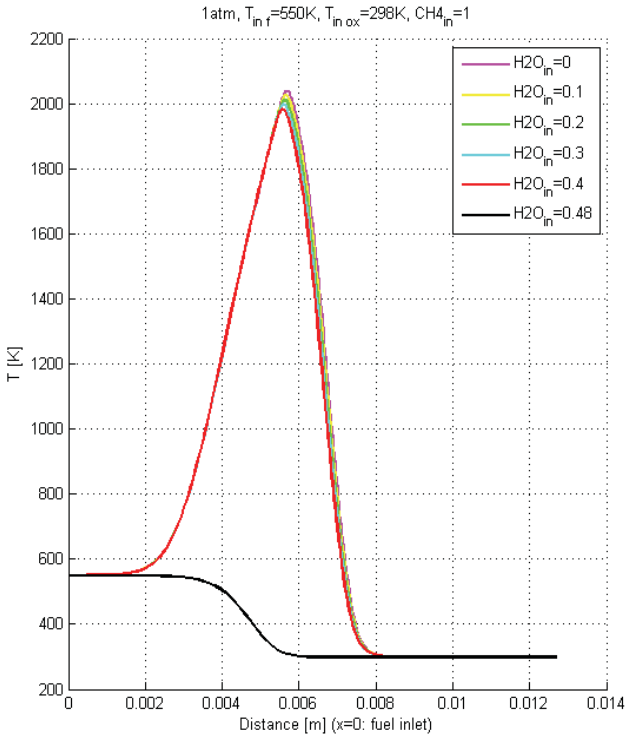

Figure 2: Temperature profile for water addition (GRI3.0), T_f_in=550 K

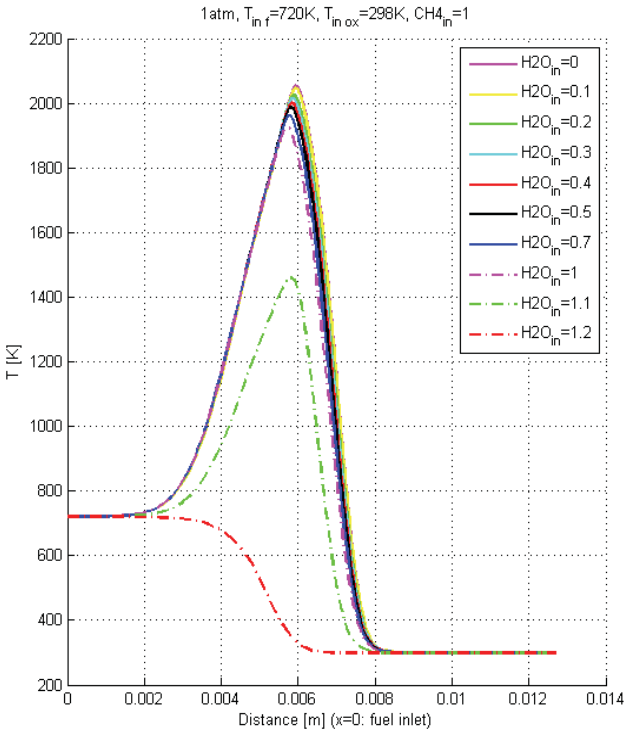

Figure 3: Temperature profile for water addition (GRI3.0), T_f_in=720 K

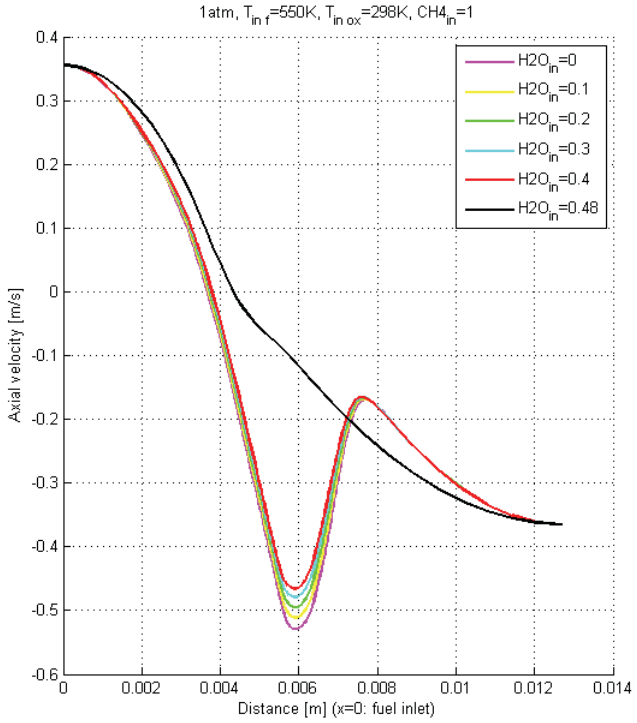

Figure 4: Temperature profile for water addition (GRI3.0), T_f_in=550 K

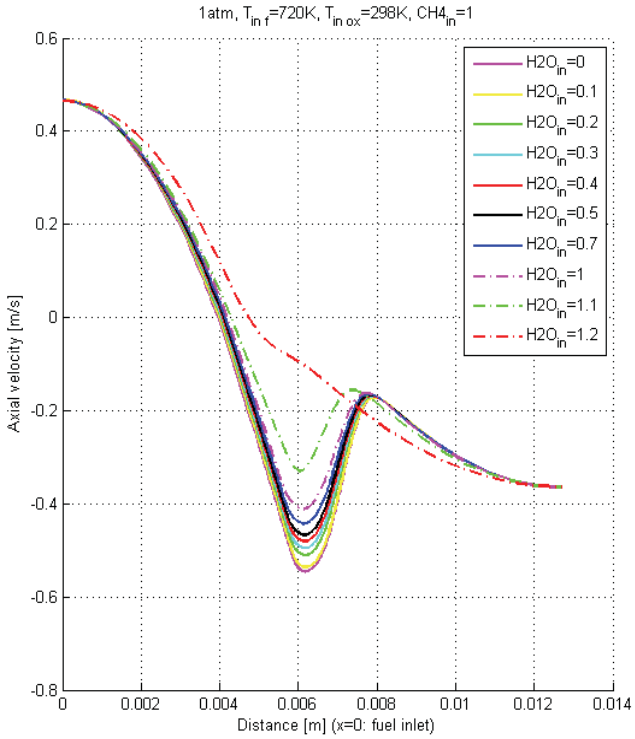

Figure 5: Temperature profile for water addition (GRI3.0), T_f_in=720 K

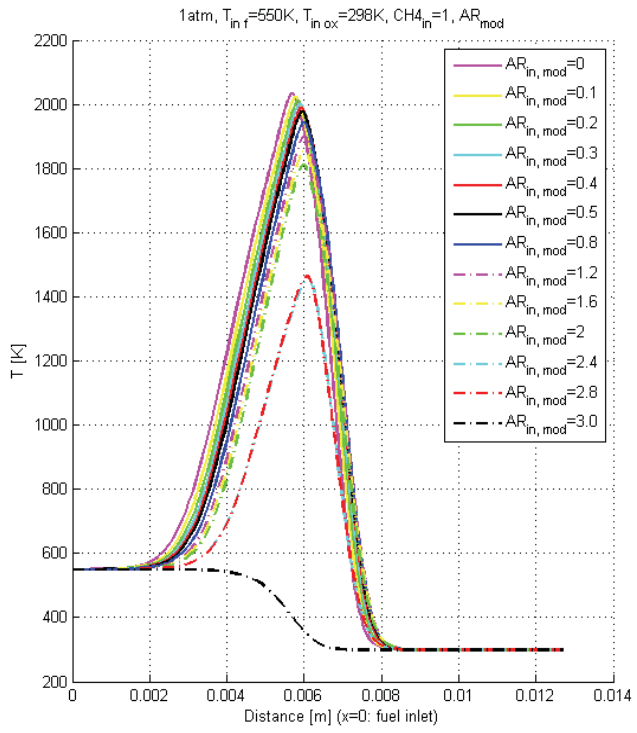

Figure 6: Temperature profile for fake AR addition (GRI3.0), T_f_in=550 K

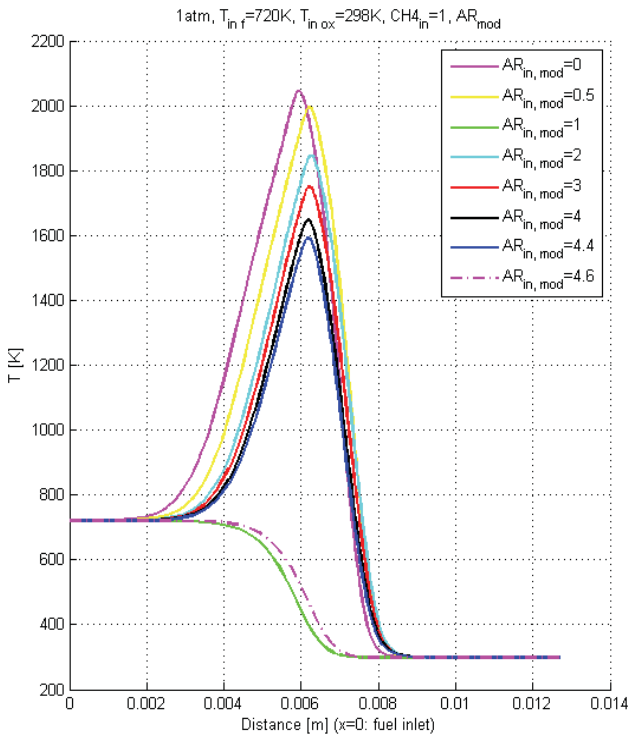

Figure 7: Temperature profile for fake AR addition (GRI3.0), T_f_in=720 K

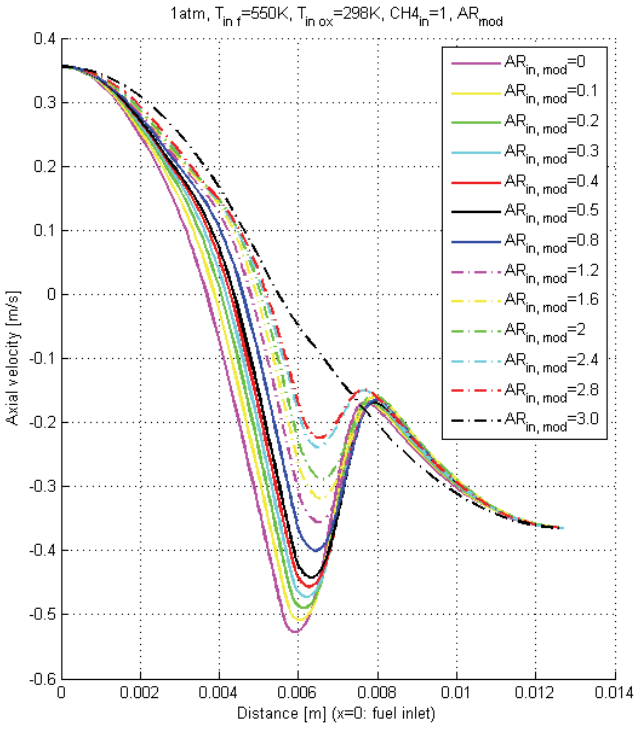

Figure 8: Temperature profile for fake AR addition (GRI3.0), T_f_in=550 K

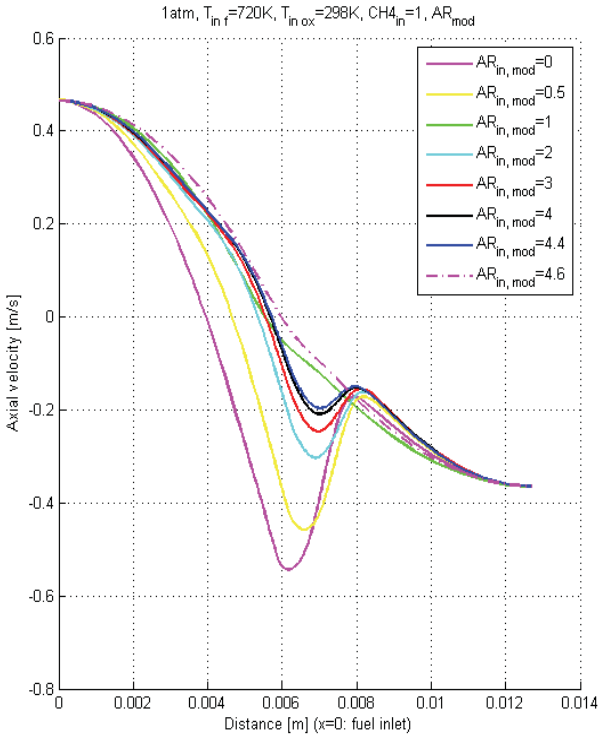

Figure 9: Temperature profile for fake AR addition (GRI3.0), T_f_in=720 K

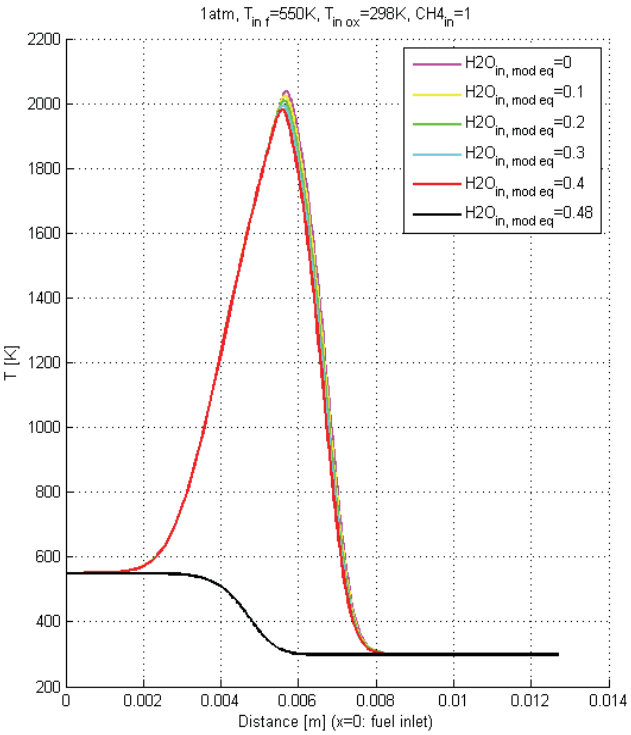

Figure 10: Temperature profile for water addition (reduced model), T_f_in=550 K

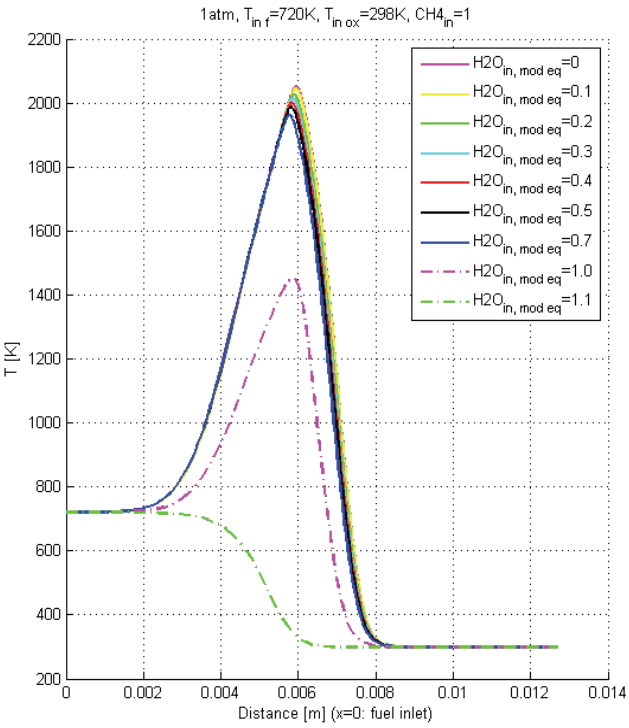

Figure 11: Temperature profile for water addition (reduced model), T_f_in=720 K

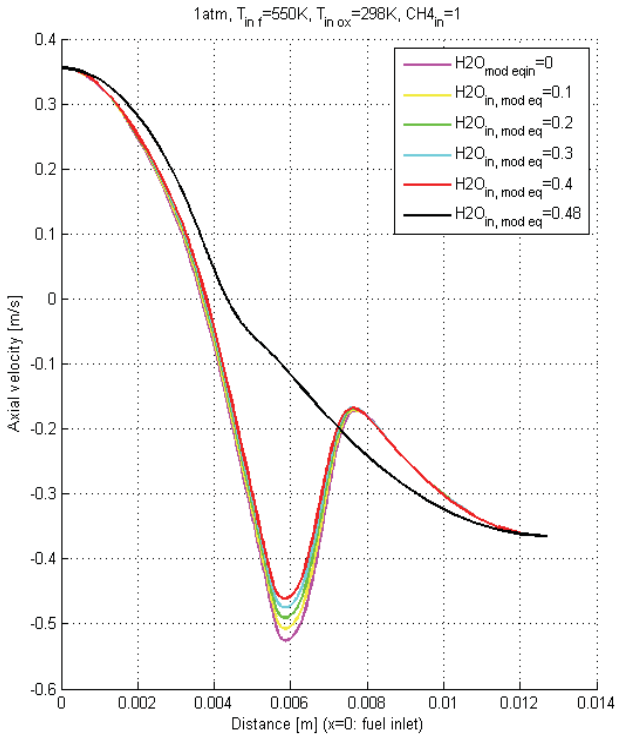

Figure 12: Axial velocity profile for water addition (reduced model), T_f_in=550 K

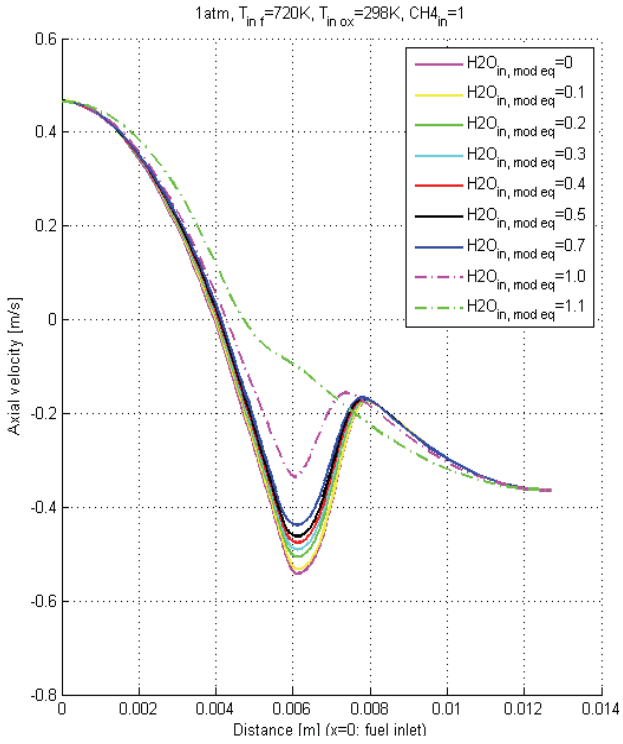

Figure 13: Axial velocity profile for water addition (reduced model), T_f_in=720 K

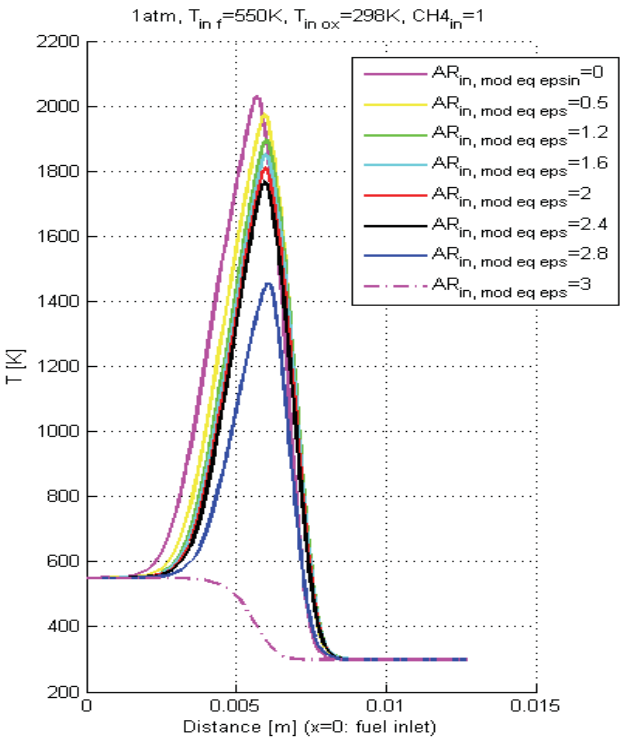

Figure 14: Temperature profile for fake AR addition (reduced model), T_f_in=550 K

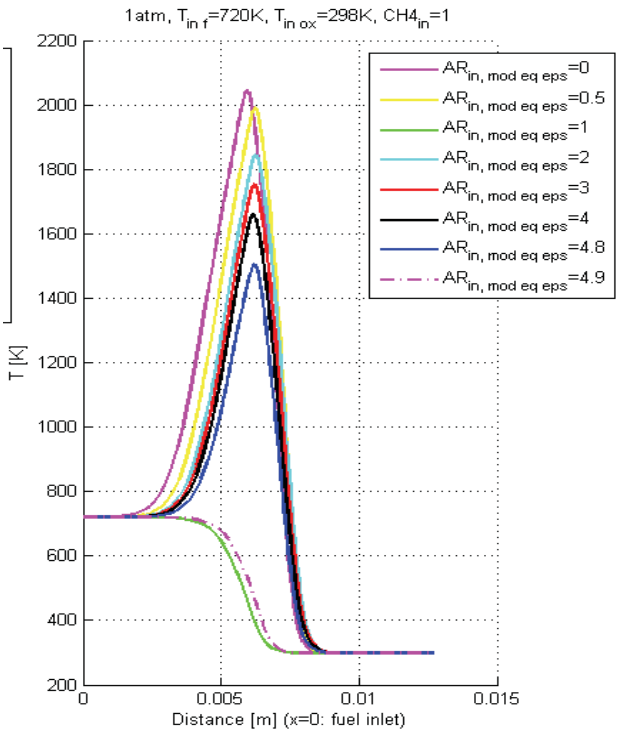

Figure 15: Temperature profile for fake AR addition (reduced model), T_f_in=720 K

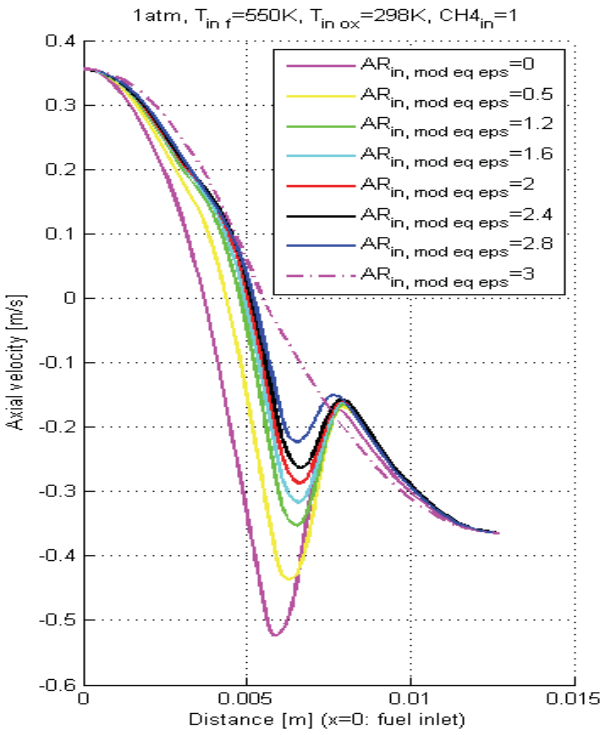

Figure 16: Axial velocity profile for fake AR addition (reduced model), T_f_in=550 K

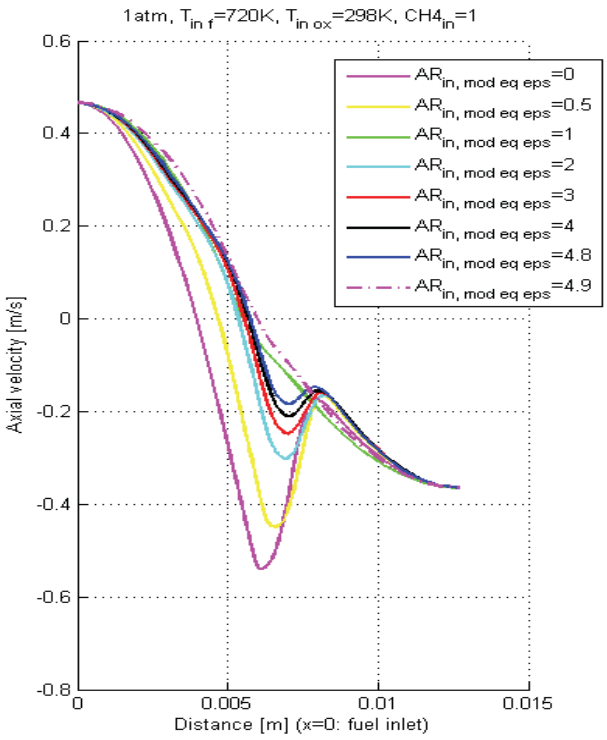

Figure 17: Axial velocity profile for fake AR addition (reduced model), T_f_in=720 K

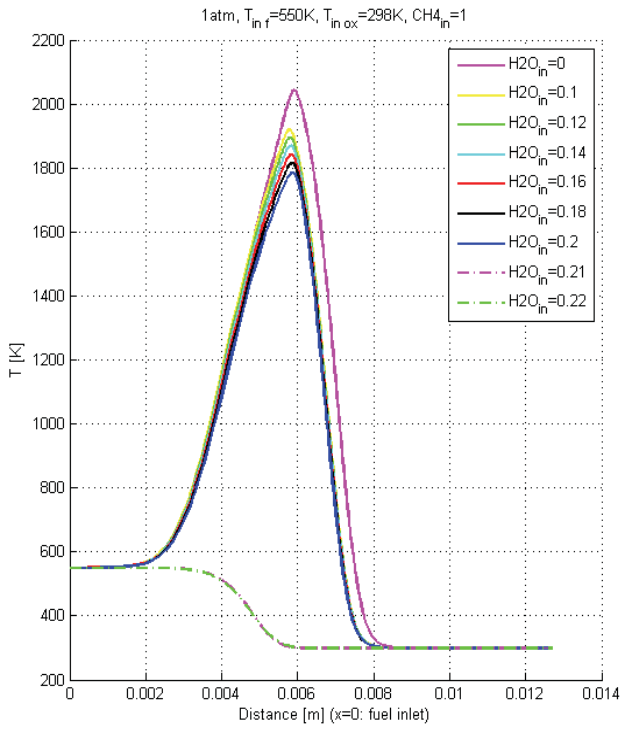

Figure 18: Temperature profile for water addition on air side (GRI3.0), T_f_in=550 K

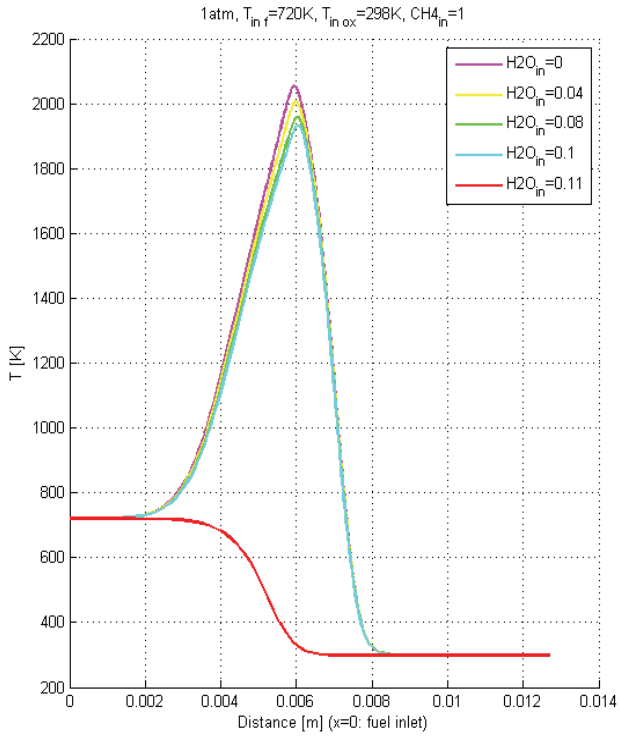

Figure 19: Temperature profile for water addition on air side (GRI3.0), T_f_in=720 K

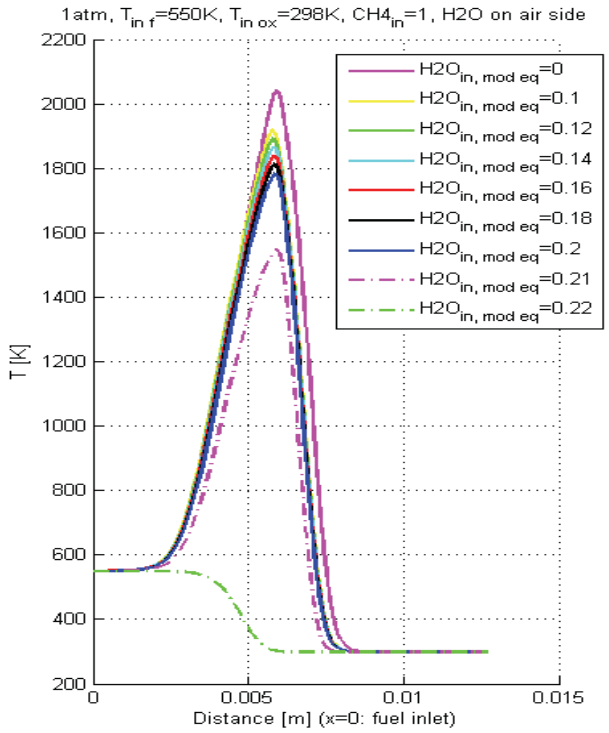

Figure 20: Temperature profile for water addition on air side (reduced model), T_f_in=550 K

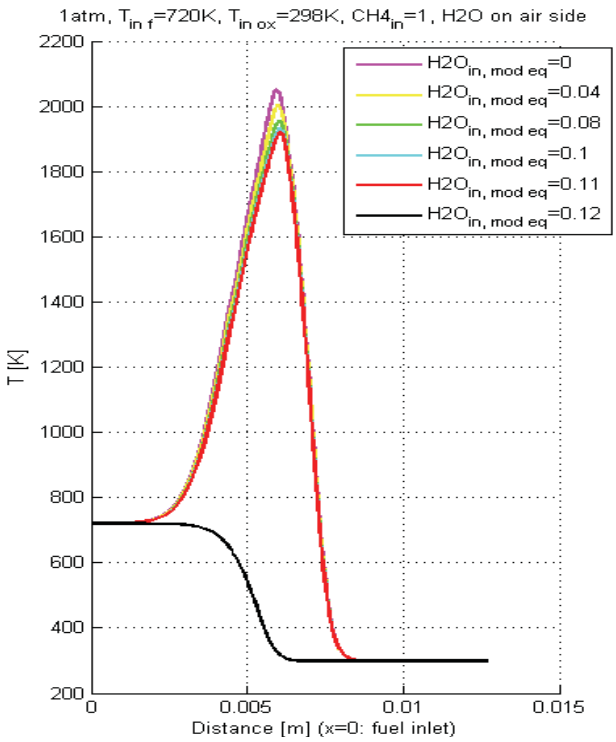

Figure 21: Temperature profile for water addition on air side (reduced model), T_f_in=720 K